Supplementary Figures

Figure S1. Four camera views in the imaging experiment.

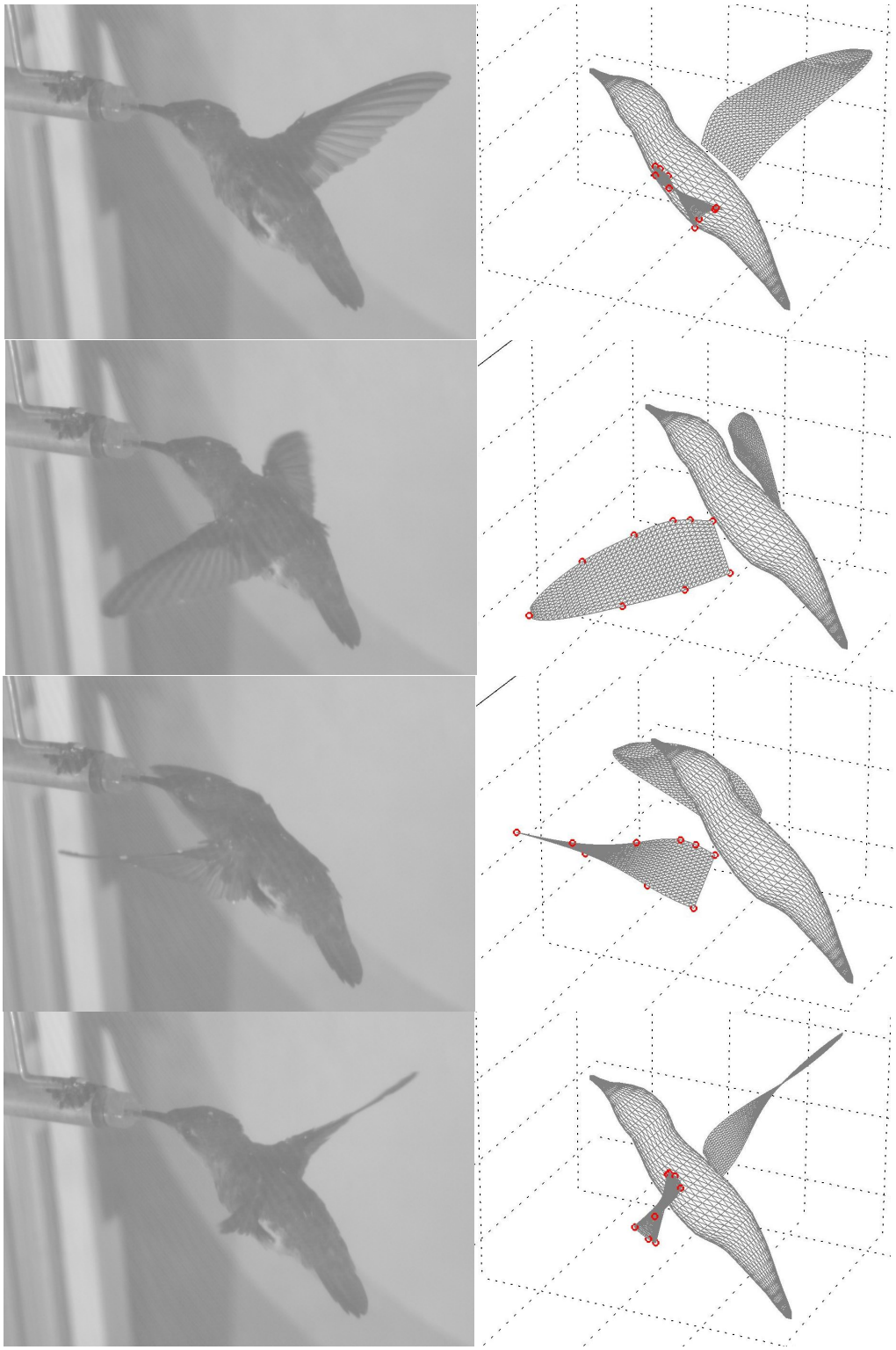

Figure S2. Comparison of the reconstructed wing and that in the video image during early downstroke, around mid-downstroke, early upstroke, and around mid-upstroke.

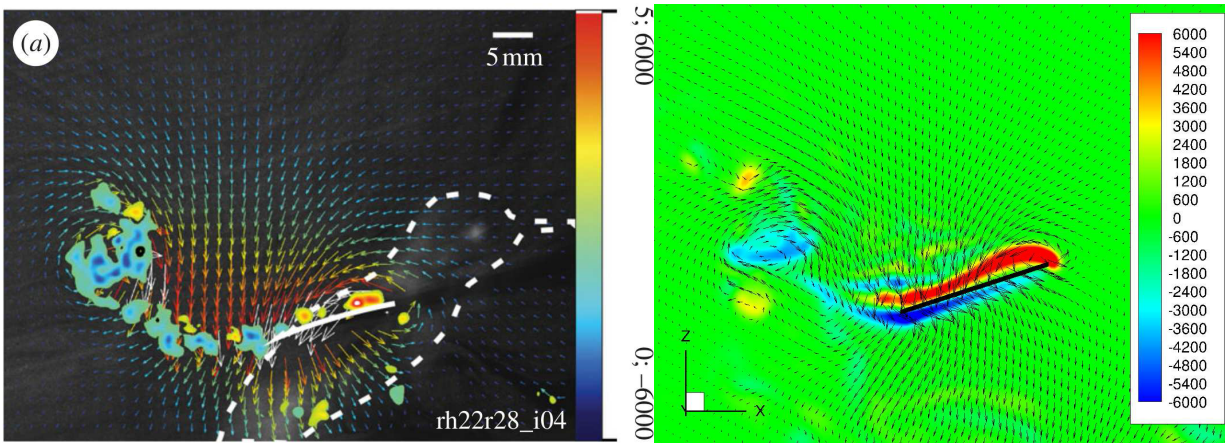

Figure S3. Flow and vorticity field during mid-downstroke from Figure 2a in Warrick et al [Ref. 10] and CFD simulation. This pair was described in the manuscript along with discussions.

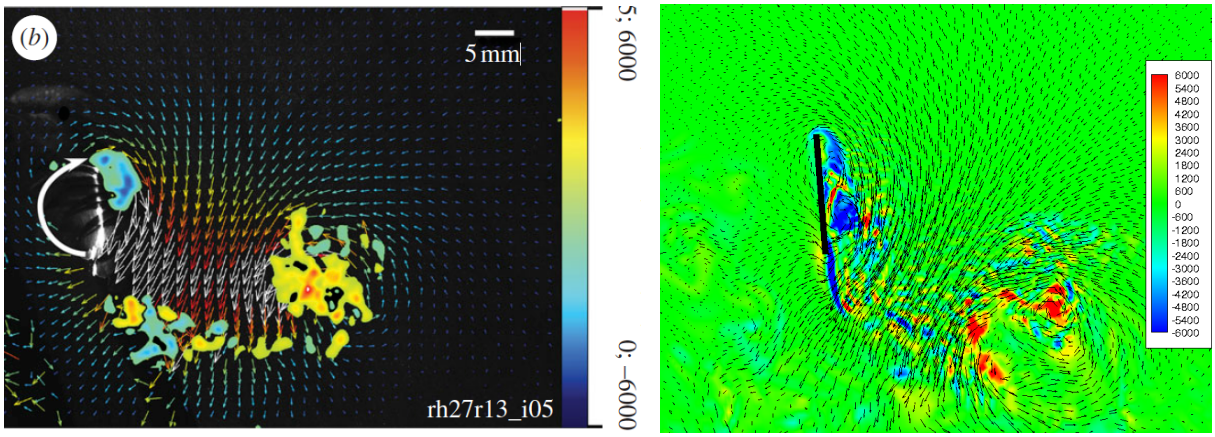

Figure S4. Flow and vorticity field during supination from Figure 2b in Warrick et al [Ref. 10] and CFD simulation. **Similarities:** A leading-edge vortex (LEV) is shown in both cases, and a large counterclockwise vortex is present about two chord lengths away from the trailing edge; clockwise flow circulation around the wing can be seen, and the main stream (on the dorsal side) goes downward and also somewhat to the left. **Differences:** In simulation the LEV extends to most of the chord; a trailing-edge vortex (TEV) sheet is seen and extends downward; this vortex sheet is likely in the shadow in experiment; the details of broken vortices are considerably different; possible noises in the velocity field can be seen in experiment at the lower left corner.

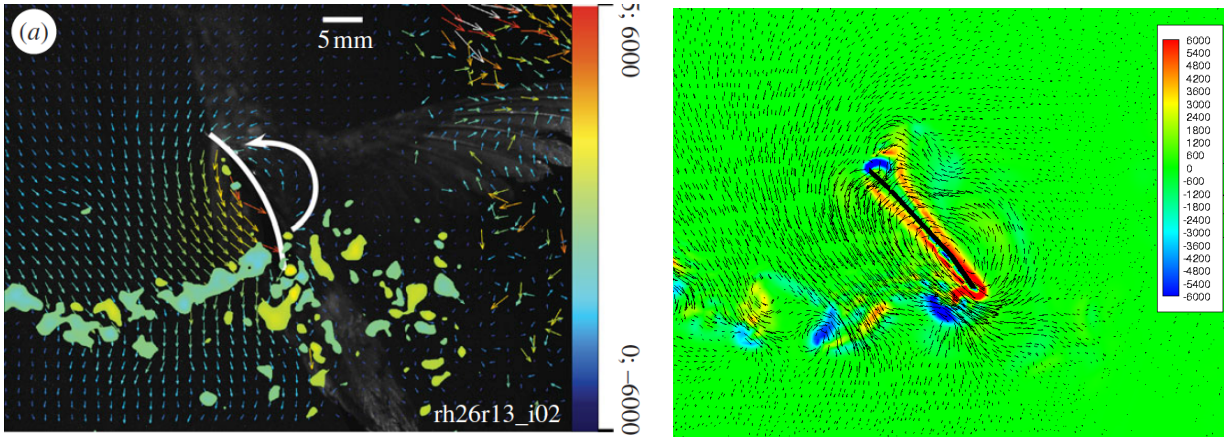

Figure S5. Flow and vorticity field during pronation from Figure 3a in Warrick et al [Ref. 10] and CFD simulation. **Similarities:** Counterclockwise flow circulation is formed around the wing, and a train of vortices are seen in the wake of the trailing edge. **Differences:** The vortex sheet on both sides of the wing surface is not visible in experiment but is present in simulation; LEV starts to form in simulation; small vortices are present on the dorsal side (right side) of the wing in experiment; the velocity field on the far right side in experiment is possibly noisy.

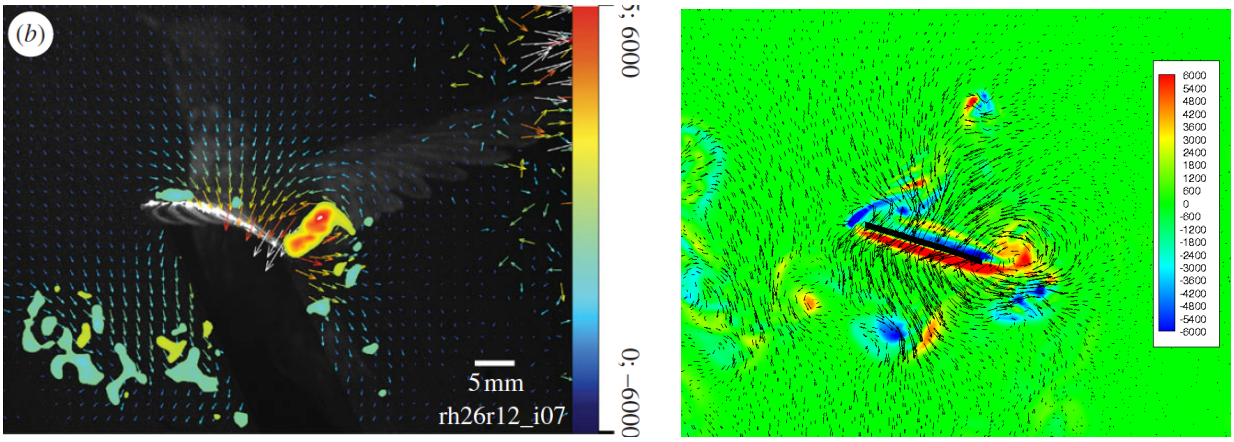

Figure S6. Flow and vorticity field shortly after pronation from Figure 3b in Warrick et al [Ref. 10] and CFD simulation. **Similarities:** Flow above the wing moves downward along with the wing; an LEV and a negative vortex sheet on the dorsal surface can be seen (though it is not very clear in experiment); a large counterclockwise vortex is forming at the trailing edge; small vortices are present in the lower left region. **Differences:** In experiment the LEV and dorsal vortex sheet are fragmented and flow below the wing is in the shadow; the wing velocity of the bird in the experiment seems to be directed more downward – likely due to variations in the wing kinematics – and thus the trailing-edge vortex is at higher elevation with respect to the wing. Velocity vectors are possibly noisy in the far right region in experiment.

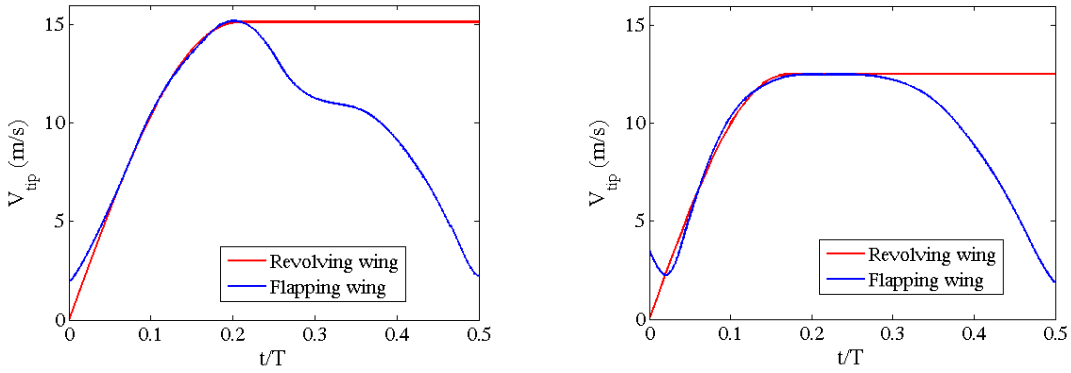

Figure S7. Comparison of the wing tip velocity between the flapping wing and revolving wing. Left: downstroke; right: upstroke. Note that for the flapping wing, the wing tip never has a moment of 'zero velocity' since the velocity vector always has a non-zero component. The acceleration period of the revolving wing is approximated with a sinusoidal function.